Research Paper

Indirect frontocingulate structural connectivity predicts clinical response to accelerated rTMS in major depressive disorder

Deborah C.W. Klooster, PhD; Iris N. Vos, BSc; Karen Caeyenberghs, PhD; Alexander Leemans, PhD; Szabolcs David, PhD; René M.H. Besseling, PhD; Albert P. Aldenkamp, PhD; Chris Baeken, MD, PhD

Published online on Jan. 28, 2020; subject to revision

Background: Repetitive transcranial magnetic stimulation (rTMS) is an established treatment for major depressive disorder (MDD), but its clinical efficacy remains rather modest. One reason for this could be that the propagation of rTMS effects via structural connections from the stimulated area to deeper brain structures (such as the cingulate cortices) is suboptimal. **Methods:** We investigated whether structural connectivity — derived from diffusion MRI data — could serve as a biomarker to predict treatment response. We hypothesized that stronger structural connections between the patient-specific stimulation position in the left dorsolateral prefrontal cortex (dlPFC) and the cingulate cortices would predict better clinical outcomes. We applied accelerated intermittent theta burst stimulation (aiTBS) to the left dlPFC in 40 patients with MDD. We correlated baseline structural connectivity, quantified using various metrics (fractional anisotropy, mean diffusivity, tract density, tract volume and number of tracts), with changes in depression severity scores after aiTBS. **Results:** Exploratory results ($p < 0.05$) showed that structural connectivity between the patient-specific stimulation site and the caudal and posterior parts of the cingulate cortex had predictive potential for clinical response to aiTBS. **Limitations:** We used the diffusion tensor to perform tractography. A main limitation was that multiple fibre directions within voxels could not be resolved, which might have led to missing connections in some patients. **Conclusion:** Stronger structural frontocingular connections may be of essence to optimally benefit from left dlPFC rTMS treatment in MDD. Even though the results are promising, further investigation with larger numbers of patients, more advanced tractography algorithms and classic daily rTMS treatment paradigms is warranted. **Clinical trial registration**: http://clinicaltrials.gov/show/NCT01832805

Introduction

Excitatory repetitive transcranial magnetic stimulation (rTMS) is a noninvasive brain stimulation technique approved by the United States Food and Drug Administration to treat (moderate) medication-resistant major depressive disorder (MDD).[1] Most frequently applied to the left dorsolateral prefrontal cortex (dlPFC), the repetitive administration of magnetic stimuli induces brain plasticity changes that outlast the period of stimulation.[2] Although this technique has shown promising results, the overall response rate to date has been rather modest for classical daily rTMS protocols. According to a meta-analysis by Berlim and colleagues,[3] the rates for response and remission are 29.3% and 18.6%, respectively. Accelerated rTMS treatment protocols (e.g., accelerated rTMS or accelerated intermittent theta burst stimulation [aiTBS]) have been evaluated for their potential to increase clinical response. Instead of the usual daily stimulation sessions, accelerated stimulation protocols involve multiple sessions per day, significantly reducing the duration of stimulation and showing similar clinical outcome rates.[4,5]

A possible explanation for the modest clinical outcomes associated with rTMS could be that for some patients the cortical stimulation region is not the best "entrance point" for affecting the underlying deregulated neurocircuitry in MDD.[6] Major depressive disorder can be considered a network disease, and the cingulate cortex in particular has been shown to be of paramount importance when it comes to treatment response.[7–11] Although the exact mechanism of action of rTMS is not yet known, there is evidence that the effects of stimulation spread throughout underlying brain networks. Fox and colleagues[8] have supported the network theory by showing functional connections between the subgenual cingulate area and the left dlPFC. Invasive and noninvasive stimulation of

Correspondence to: D.C.W. Klooster, Eindhoven University of Technology, Department of Electrical Engineering, Building Flux, Office 5.084, De Groene Loper 19, 5612 AZ Eindhoven, the Netherlands; d.c.w.klooster@tue.nl

Submitted Apr. 30, 2019; Revised July 23, 2019; Accepted Aug. 27, 2019

DOI: 10.1503/jpn.190088

these brain areas have shown clinical effects in patients with depression. Furthermore, it has been stated that preserved frontocingulate neurocircuitries may be of essence to optimally benefit from left dlPFC neurostimulation.[6,12]

So far, the potential link between structural connections and clinical response to brain stimulation has not yet been investigated. However, Amico and colleagues[13] showed correlations between structural connections and the effects of transcranial magnetic stimulation (TMS), as measured by TMS-evoked potentials in electroencephalography, suggesting that the effects of stimulation propagate throughout the brain via structural connections. Furthermore, structural connections may play a role in clinical efficacy.[6,12,13]

In this study, we investigated the importance of structural connectivity, estimated using diffusion MRI (dMRI), for the clinical effectiveness of aiTBS. Using various gradient directions during MRI scanning, it is possible to map the direction in which water diffusion is least restricted, to derive a so-called diffusion tensor.[14,15] The application of tractography algorithms allows the assumed spatial orientation of anatomic (structural) connections between different brain areas to be reconstructed. We evaluated whether individual baseline structural connectivity between the stimulated area (left dlPFC) and the cingulate cortices could be of predictive value for clinical response to aiTBS in patients with MDD.[7] Specifically, we hypothesized that stronger baseline structural connections between the stimulated area and the cingulate cortex would be associated with better clinical response.

Methods

The current study (http://clinicaltrials.gov/show/NCT01832805) was approved by the Ghent University Hospital ethics committee and conducted in accordance with the declaration of Helsinki (2004). All patients gave written informed consent.

Patient inclusion

Fifty right-handed patients with MDD were included in this clinical aiTBS study. We diagnosed MDD using the structured Mini-International Neuropsychiatric Interview.[16] All patients were at least stage I treatment-resistant. They had a minimum of 1 unsuccessful treatment trial with selective serotonin reuptake inhibitors or serotonin and norepinephrine reuptake inhibitors. Medication was tapered off, and all patients were at least 2 weeks antidepressant-free before stimulation. More extensive information about patients and clinical outcomes can be found in a study by Duprat and colleagues.[17]

Study protocol

The overall design of this randomized, double-blind, sham-controlled, crossover trial is shown in Appendix 1, available at jpn.ca/190088-a1. Patients were randomized to receive sham aiTBS first, followed by active aiTBS (arm A) or the other way around (arm B) (Appendix 1, Fig. S1. We used only the baseline dMRI data to investigate our hypothesis.

All patients first underwent baseline MRI (3 T Siemens TrioTim) on day 1 (T1) with anatomic imaging (magnetization prepared rapid acquisition gradient echo [MPRAGE]; repetition time 2530 ms, echo time 2.58 ms, flip angle 7°, field of view 220 × 220 mm^2, resolution 0.9 × 0.9 × 0.9 mm^3, 176 slices), and we acquired dMRI scans using a single-shot echo planar imaging sequence (repetition time 8500 ms, echo time 85 ms, field of view 244 × 244 mm^2, voxel size 2 × 2 × 2 mm^3, 68 slices, acquisition time 9.14 min). For every patient, we acquired 62 diffusion-weighted images: 60 images with b = 800 s/mm^2 (30 noncolinear gradient directions, 2 averages) and 2 b_0 images.

We used a Magstim Rapid^2 Plus^1 magnetic stimulator (Magstim Company Limited) connected to an active or sham figure-8-shaped coil (Magstim 70 mm double air film [sham] coil) to apply the active and sham stimulations. The left dlPFC, defined as the centre part of the midprefrontal gyrus (Brodmann area 9/46) based on anatomic MRI of each person,[18] was stimulated at 110% of the resting motor threshold. Positioning of the coil (45° anterolateral) was maintained using the BrainSight neuronavigation system (Rogue Resolutions, Inc). According to the accelerated protocol, we administered 5 stimulation sessions per day on 4 consecutive days (days 2 to 5, and days 9 to 12). One iTBS session consisted of 54 trains of 2 s of stimulation given in an 8 s cycling period. During the 2 s, 10 bursts of 3 stimuli were given. This added up to 1620 stimuli per session, for a total of 32 400 stimuli over the 4-day treatment period. Between sessions, patients had breaks of approximately 15 minutes. During stimulation, patients were blindfolded, wore earplugs and were kept unaware of the type of stimulation (sham or active) they received.

Analysis pipeline

We used MRIcron to loop through the raw diffusion-weighted MRI data in different orthogonal views to look for obvious artifacts (e.g., large signal dropouts, geometric distortions, zebra artifacts). We used the quality assessment toolbox from FreeSurfer (version 6.0.0; https://surfer.nmr.mgh.harvard.edu/fswiki/QATools) to check the (sub)cortical segmentation quality of the MPRAGE data and Freeview to loop through the image maps in multiple planes.

We analyzed the dMRI data sets using ExploreDTI[19] (version 4.8.6). First, we masked the FreeSurfer data sets from T1 with ExploreDTI (kernel size of morphological operators = 5; intensity threshold 5%). Then, we corrected the dMRI data for signal drift, subject motion, eddy-current-induced distortions and susceptibility artifacts,[20–22] with the masked data sets from T1 as undistorted (target) scans. We performed quality assessment of the corrected dMRI data for every patient. We checked the colour-coded fractional anisotropy (FA) maps of the preprocessed data and the residuals maps. Data were marked as "low quality" when the FA colours were incorrect or scattered, or when the average residuals showed low fit of the diffusion tensor and when the outliers had high peaks. As well, the diffusion data set was excluded from further analysis if the translational motion exceeded the

voxel size (2 mm^3). More detailed information can be found in Caeyenberghs and colleagues.[23,24]

We estimated the diffusion tensor from the corrected images with the robust fitting routine REKINDLE[25,26] before applying whole-brain tractography[27] with a uniform seed point resolution of 2 mm^3, a step size of 1 mm, an angle threshold of 30° and an FA threshold of 0.2.

Fibre paths of interest

We used FreeSurfer to parcellate the anatomic data sets according to the Desikan–Killiany parcellation scheme[28] in 68 cortical and 19 subcortical nodes (cerebellum, thalamus, caudate, putamen, pallidum, hippocampus, amygdala, accumbens area and ventral diencephalon bilaterally, as well as the brainstem). We also added 2 nodes representing the patient-specific stimulation site and the subgenual anterior cingulate cortex (sgACC). The node representing the patient-specific stimulation site was defined as the grey matter parts of a circular region of interest (ROI) with a radius of 12 mm that was placed over the patient-specific stimulation site, as saved in the BrainSight neuronavigation system. The radius was derived from the linear decay of metabolic changes seen in animal TMS experiments.[29,30] Because 1 voxel cannot belong to multiple nodes, voxels in the stimulation-site node were subtracted from the Desikan–Killiany node they originally belonged to. The sgACC node was defined as the grey matter parts of a circular ROI at Montreal Neurological Institute position $x = 6$, $y = 16$, $z = -10$ (converted to the patient's native space using inverse normalization matrices) with a radius of 10 mm, as used by Fox and colleagues.[10] This resulted in 89 nodes for structural connectivity analysis.

We used ExploreDTI to calculate connectivity matrices between the 89 nodes. Specifically, only the tracts that actually ended within the nodes were taken into account. We performed manual inspection to confirm that there were no loose fibres in our tracts. We derived the label file from the Desikan–Killiany label template as provided by ExploreDTI (FS_cvs_avg35_inMNI152_aparc+aseg_E_DTI_label_names.txt). See Figure 1 for an overview of the analysis steps.

According to our hypothesis, parts of the cingulate cortex are responsible for the clinical efficacy of brain stimulation treatment. According to the Desikan–Killiany atlas, the cingulate cortex is split into 4 parts bilaterally: isthmus, posterior, caudal and rostral (Fig. 2). The rostral and caudal parts refer to the anterior cingulate cortex. We used the 8 cingulate cortex regions plus the sgACC for a total of 9 ROIs in this study.

First, we investigated the existence of a direct structural connection between the stimulated position in the left dlPFC and any of the ROIs. We also investigated potential indirect pathways, with a focus on those with 1 or 2 nodes that connected the stimulation site in the dlPFC to either of the ROIs in the cingulate cortex, further referred to as internodes.

Quantification of structural connectivity

Examples of fibre tracts between specific sets of nodes can be seen in Figure 3**.** We used various metrics to quantify structural connectivity between the stimulation position in the left dlPFC

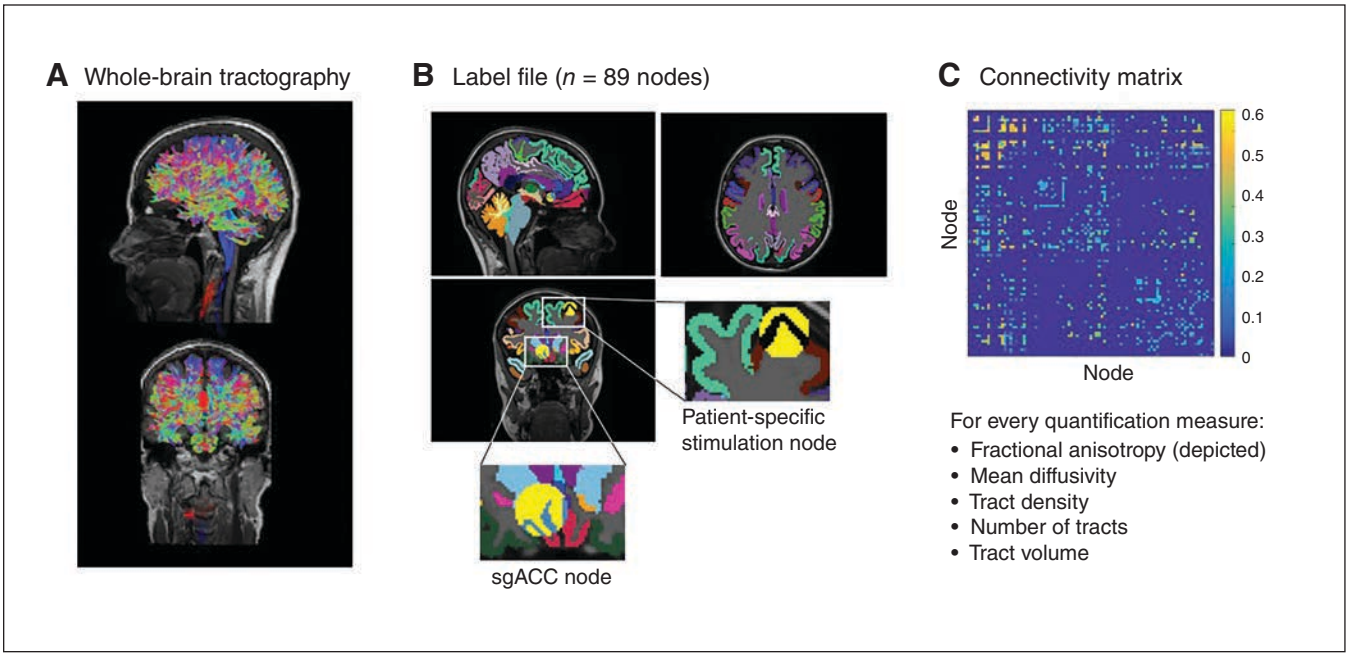

Fig. 1: (A) We obtained whole-brain tractography results using ExploreDTI. (B) The label file contained 89 nodes. We manually added circular regions of interest surrounding the patient-specific stimulation position and the subgenual anterior cingulate cortex (sgACC; yellow nodes). We used the grey matter parts of these regions of interest as the patient-specific stimulation node and the sgACC node (shown in black and grey, respectively). (C) We computed connectivity matrices using multiple quantification measures.

and the predefined ROIs: number of tracts, volume of tracts, tract density (TD), FA and mean diffusivity (MD). The number of tracts, between nodes u and v for example, represented the number of tracts starting in u and ending in v (or vice versa). We calculated the total volume of these tracts as the volume (voxels) intersected by these streamlines. Tract density[31] is the number of connections per unit surface (e.g., mean area of nodes u and node v). The FA and MD values[27] are measures of anisotropy and trace of the diffusion tensor, respectively.

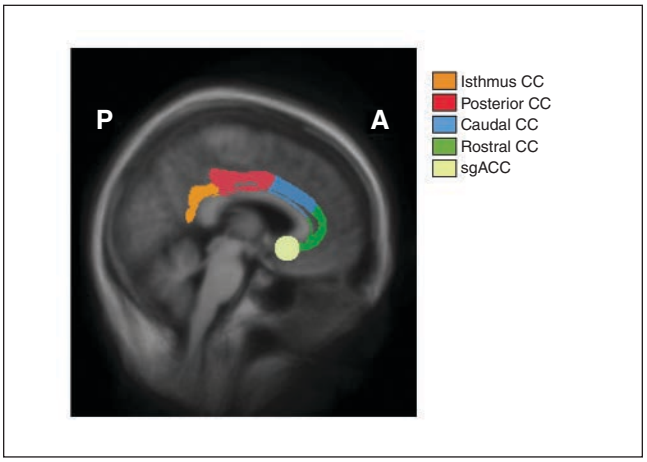

Fig. 2: Nine regions of interest in the cingulate cortex: the isthmus, posterior, caudal and rostral (bilaterally) were derived from the Desikan–Killiany atlas. The subgenual anterior cingulate cortex (sgACC) was added manually. A = anterior; CC = cingulate cortex; P = posterior.

We quantified the pathways between the stimulation site and the ROIs according to a formula derived from the definition of path length from graph theory. Path length is a measure of integration and is defined as the shortest path (distance, d) between 2 nodes.[32,33]

$$dPath_{dlPFC-ROI} = \sum_{a_{uv} \in g^{w}_{dlPFC \leftrightarrow ROI}} f(SC_{uv})$$

$$f(SC_{uv}) = \frac{1}{SC_{uv}}$$

In the equations above, f represents the inverse transformation from weight to distance, as described by the various structural connectivity (SC) metrics. The stronger the structural connection, the shorter the distance. The undirected, weighted path from the dlPFC to an ROI is represented by $g^{w}_{dlPFC \leftrightarrow target}$. Because this represents an indirect pathway, it is quantified by summing the structural characteristics of the sub-paths between the dlPFC and the ROI, a_{uv}. Specifically, in cases of 1 internode, there are 2 sub-paths: from the dlPFC to the internode (u = dlPFC, v = internode), and from the internode to the ROI (u = internode, v = ROI). In cases of 2 internodes, there are 3 steps. Beyond the single (shortest) pathway between 2 nodes, currently defined as the path length, we averaged all possible pathways between the dlPFC and the ROIs, assuming that neuronal communication is not restricted to a single pathway. Therefore, the final metric to quantify the structural connection between the dlPFC and the ROI was named "total distance" (*dTot*) and defined as follows:

$$dTot_{dlPFC-ROI} = \frac{1}{nrpathways} \sum_{i=1}^{nrpathways} dPath_{dlPFC-ROI(pathway_i)}$$

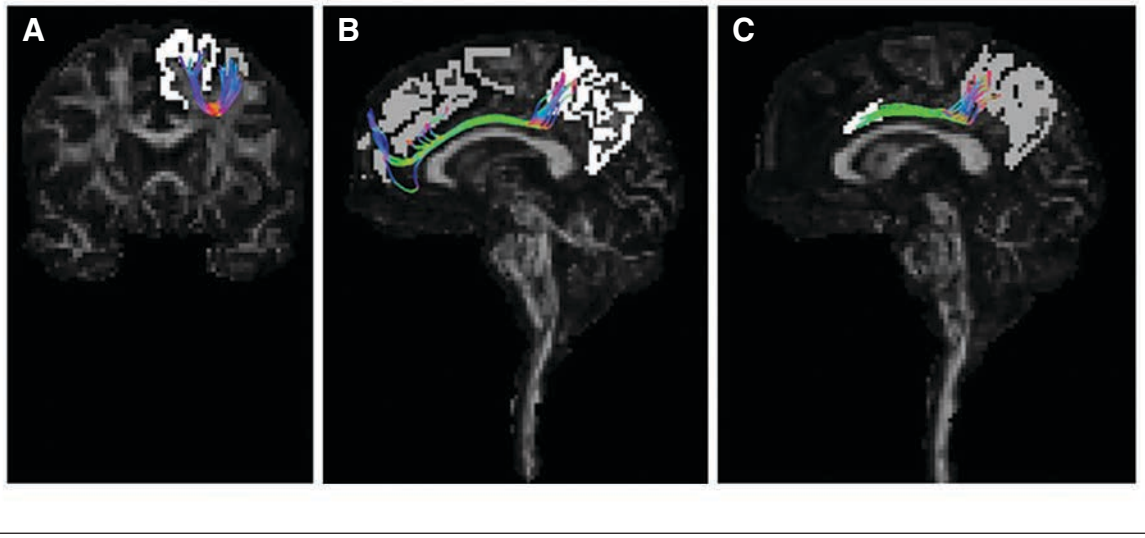

Fig. 3: Example of a pathway between the stimulation position and the left caudal part of the cingulate cortex via the left superior frontal cortex. (A) The structural connection between the patient-specific stimulation site in the left dorsolateral prefrontal cortex and the first internode, in this case the superior frontal cortex. (B) The connection between the first and second internodes. (C) The connection between the second internode and the caudal part of the cingulate cortex. The fractional anisotropy map is used as template, and the nodes are shown in grey and white. Note that in each panel, the pathway is from the grey node to the white node. For example, the white node in (A) is the grey node in (B). The same holds for (B) and (C). Different colours represent different directions of neuronal pathways: green = anterior–posterior; red = left–right; blue = inferior–superior.

Note that this general measure can be derived from 5 different structural connectivity quantification measures: number of tracts, volume of tracts, tract density, FA and MD.

Specificity to frontocingulate structural connectivity

To investigate whether the specific structural connectivity between the stimulation position and the cingulate cortex was important for predicting clinical response to aiTBS (and not the overall whole-brain structural connectivity strength) we derived 3 additional measures from the baseline whole-brain tractography results. We correlated the total number of tracts and whole-brain FA and MD values with the changes in score on the Hamilton Depression Rating Scale (HDRS).[34] We calculated whole-brain FA and MD values as the sum of the average FA or MD values in every tract.

We also computed nodal structural connectivity measures for the stimulation region. We calculated the average FA and MD values in the stimulation node, as well as average FA and MD values for the connections from the stimulation node to all other nodes in the brain. We also computed the total number of tracts starting from the stimulation region, together with the total volume of these tracts. We then correlated nodal structural connectivity measures with clinical responses.

Group analysis

To investigate whether specific individual structural characteristics are important for correlations with clinical response, we repeated the analysis using a group connectome using data from our 40 depressed patients. Because the patient-specific stimulation sites were added as nodes in this analysis, it was not possible to average the connectivity matrices over all patients to obtain an average structural group connectome. Therefore, we coregistered an individual patient's specific stimulation site to the native space of all other patients to create an 89 × 89 patient-specific average connectivity matrix. We repeated this process for each participant, resulting in 40 patient-specific average connectivity matrices, each differing in only 1 node: the respective stimulation site for the individual patient (see Appendix 1 for more details). We did not take the sgACC into account for the group analysis, because only 9 patients showed indirect structural connections, using 2 internodes, from the stimulation position in the left dlPFC to the sgACC.

Statistical analysis

Because our previous results[17] clearly showed that the clinical effects of aiTBS treatment had a delayed onset, we focused on clinical outcomes at T4, defined as $\Delta HDRS_{del} = HDRS_{T4} - HDRS_{T1}$. These ΔHDRS scores were correlated with $dTot_{dlFPC-target}$ values, derived from different structural connectivity metrics based on individual data and on group connectome data. Significance was set at $p < 0.05$ (2-tailed).

We also computed the prediction of the immediate effect (3 d after the first 20 sessions; T2) of the sham and active aiTBS stimulations. We measured the immediate clinical effects by the change in HDRS before and directly after the sham and active stimulation ($\Delta HDRS_{imm/sham} = HDRS_{T2} - HDRS_{T1}$; arms A and B, Appendix 1, Fig. S1). To avoid potential carryover effects, we considered only data between T1 and T2 to calculate immediate stimulation effects. The statistical approach was similar to that described for prediction of delayed effects.

Results

Four patients dropped out of the study, and 1 patient retrospectively received an altered diagnosis. Furthermore, in 2 patients the stimulation position was not saved, restricting the performance of this method. In the remaining 43 data sets, we found poor data quality owing to severe head motion in 1 patient (exceeding the size of 1 voxel) and owing to artifacts in 2 other patients. In the end, 40 dMRI data sets were included for analysis.

Structural pathways between the left dlPFC and the cingulate cortices

Given that we found no direct structural connections between the stimulated left dlPFC and any of the ROIs, and less than half of the participants showed indirect connections with 1 internode to any of the ROIs, we focused on pathways with up to 2 internodes. We detected 20 nodes as first internodes; the left superior frontal cortex was the most common (number of participants who showed left superior frontal cortex as the first internode in the indirect pathway to any of the ROIs in the cingulate cortex, mean ± standard deviation [SD] = 15.56 ± 5.66). Distribution of the second internode was slightly more widespread (n = 28). The most common observed second internodes were the bilateral superior frontal cortex (mean ± SD; left 9.78 ± 7.10; right 12.44 ± 8.76) and the bilateral precuneus (mean ± SD; left 8.67 ± 7.43; right 7.33 ± 5.69). A full overview of the distribution of the first and second internodes can be found in Appendix 1. An example of the pathway between the stimulation position and the caudal part of the cingulate cortex in the left hemisphere in a single random patient is shown in Figure 3.

Significant correlations between structural connectivity and clinical response

We used data from all patients (n = 40, arms A and B) to calculate the potential for structural connectivity to predict clinical response to aiTBS. Even when 2 internodes were considered, not all patients showed indirect structural connections between the stimulated left dlPFC and the ROIs in the cingulate cortex. The results for this section are based on a subgroup of patients who showed structural pathways between the stimulated area in the left dlPFC and the ROIs in the cingulate cortex (see Table 1 and Appendix 1 for more detailed information).

Structural connectivity, described by 3 of 5 metrics (number of tracts, volume of tracts, MD), between the left dlPFC

Table 1: Number of patients* who showed indirect structural connections, with up to 2 internodes, between the stimulation site in the left dlPFC and ROIs in the cingulate cortex

		Left cingulate cortex				Right cingulate cortex			
	sgACC	Rostral	Caudal	Posterior	Isthmus	Rostral	Caudal	Posterior	Isthmus
Number of patients	9	20	34	34	38	24	33	33	37

dlPFC = dorsolateral prefrontal cortex; ROI = region of interest; sgACC = subgenual anterior cingulate cortex.
*Out of a total of 40.

and the right caudal part of the cingulate cortex showed significant correlation ($p < 0.05$, uncorrected) with the clinical response to aiTBS. As well, the number of tracts between the stimulation position and the left posterior part of the cingulate showed predictive value. An overview is provided in Figure 4, and additional statistical details can be found in Table 2. In all cases, positive correlations indicate that lower *dTot* values (i.e., stronger structural connections) result in better clinical responses.

Clinical response prediction based on whole-brain or nodal structural connectivity metrics

Whole-brain structural connectivity metrics, total number of tracts, FA and MD, did not show significant correlation ($p < 0.05$, uncorrected) with clinical response to aiTBS. We also found no significant correlations between the nodal structural connectivity measures and clinical response. More detailed results can be found in Appendix 1.

Results using group depression connectome

Using group connectome data derived from 40 dMRI data sets from patients with depression, we found no significant correlations ($p < 0.05$, uncorrected) for baseline structural connectivity between the stimulation area in the left dlPFC and any of the ROIs in the cingulate cortex and clinical response to aiTBS.

Discussion

To our knowledge, this was the first study to use dMRI data to predict the clinical efficacy of an aiTBS treatment protocol in patients with MDD. Baseline structural connectivity between the patient-specific stimulation site in the left dlPFC and the right caudal and left posterior parts of the cingulate cortex showed predictive value for clinical response to aiTBS treatment.

One of our major findings was the absence of direct structural pathways between the stimulated area in the left dlPFC and any of the cingulate cortices. Although various neuroimaging techniques have shown functional crosstalk between the dlPFC and the cingulate cortex,[9–12,35] functional connections are not always represented by direct structural connections. Honey and colleagues[36] reasoned that this unambiguity might be explained by indirect connections, mediated by a third brain region. As well, Roge and colleagues[37] and Deligianni and colleagues[38] demonstrated that functional connections can be predicted by indirect structural connections up to the second order (i.e., indirect pathways with 2 internodes). In line with these findings, we investigated structural pathways between the left dlPFC and the cingulate cortex with up to 2 internodes. Our analyses showed that the stimulation position displayed more indirect structural connections bilaterally to the caudal and posterior parts of the cingulate cortex and the isthmus than to the rostral parts (Appendix 1). In particular, the structural connections to the caudal and posterior parts of the cingulate cortex showed predictive value for clinical response to aiTBS. These findings could not be caused by overall structural connectivity strength, because whole-brain structural connectivity metrics were not significantly correlated with clinical response.

Clinical outcome was related to structural connections from the left dlPFC to the right caudal part of the cingulate cortex, derived from the number of tracts, volume of tracts and MD. As well, we found positive correlations between *dTot*, derived from MD, between the dlPFC and the left posterior cingulate cortex. Mean diffusivity is a measure of overall diffusivity[39] and can be interpreted as an inverse measure of membrane density:[40] the more membranes in a voxel, the lower the diffusion and the lower the MD. The positive correlation indicates that lower *dTot* values (resulting from higher MD values, more tracts and a higher volume of tracts) result in better clinical response. Here, one can speculate that because of higher values, the effect of stimulation can propagate more easily to deeper structures, in this case the right caudal and left posterior cingulate cortex.

The caudal and posterior parts of the cingulate cortex have been linked to response to MDD treatment. For example, Baeken and colleagues[12] showed that higher baseline metabolic activity in the dlPFC and the entire anterior cingulate cortex, including the caudal part, were associated with better clinical outcomes. More specifically, metabolic activity in the right caudal part of the cingulate cortex has been linked to the clinical effectiveness of rTMS in a single-photo emission computerized tomography study.[35] Lozano and colleagues[9] showed increased metabolism in the posterior cingulate after deep brain stimulation to the subgenual cingulate region in 8 responders.

Biomarkers derived from individual data versus group connectome data

The fact that we found no significant correlations between baseline structural connectivity and the clinical effects of aiTBS for the group connectome may emphasize the importance of using individual structural connectivity data.

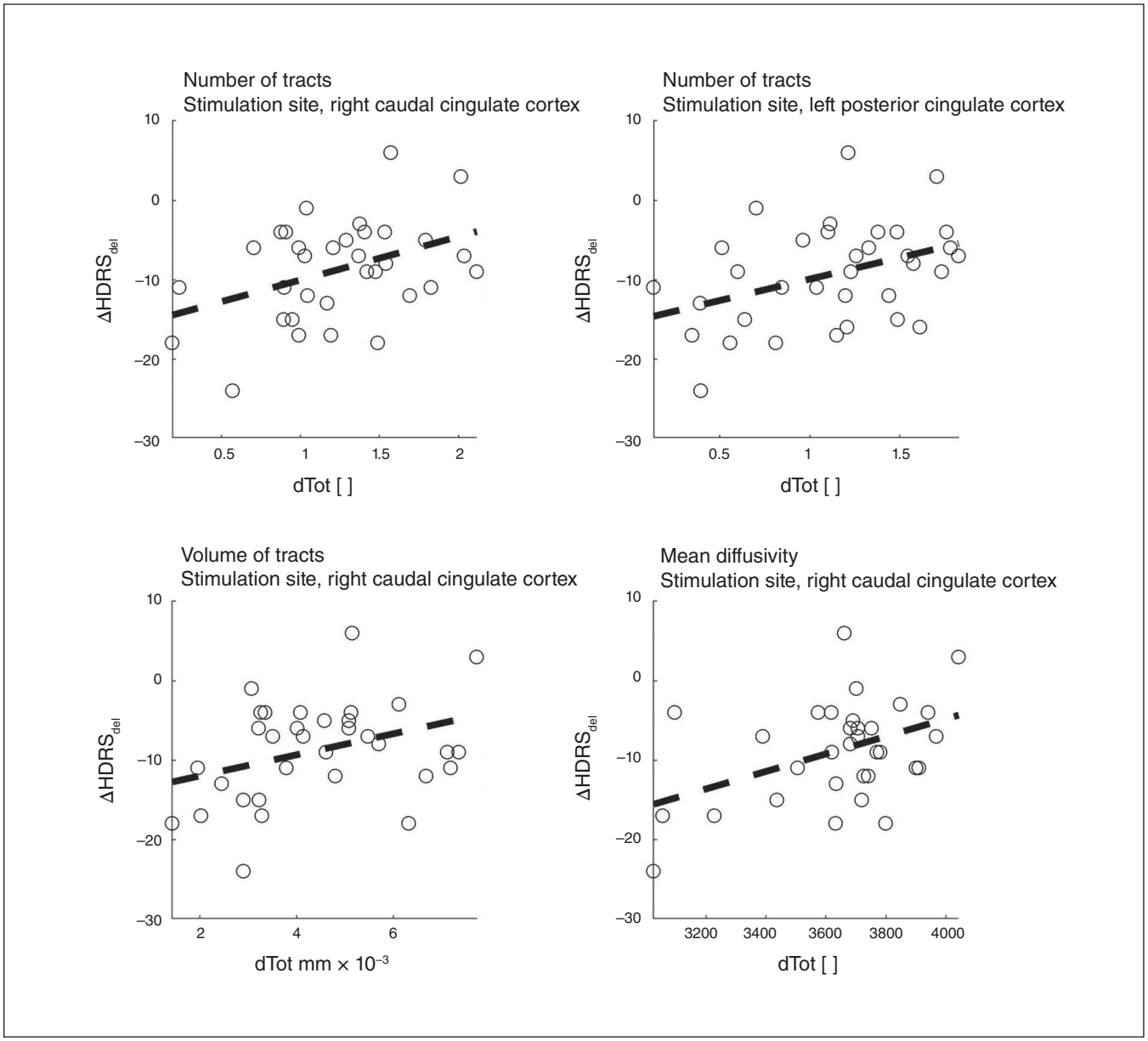

Fig. 4: Overview of the significant correlations ($p < 0.05$, uncorrected) for the baseline structural connectivity between the stimulation position in the left dorsolateral prefrontal cortex and different parts of the cingulate cortex and the delayed clinical response ($\Delta HDRS_{del}$) to accelerated intermittent theta burst stimulation, measured at T4 (2 weeks after the stimulation protocol). We found that *dTot*, calculated using the number of tracts, volume of tracts and mean diffusivity, between the stimulation site and the right caudal cingulate cortex region were significantly correlated with clinical response. As well, the *dTot* derived from the number of tracts between the stimulation site and left posterior cingulate cortex was significantly correlated. Statistical details can be found in Table 2. *dTot* = total distance; HDRS = Hamilton Depression Rating Scale.

Although tractography permits the reconstruction of white matter pathways in vivo, the accuracy of these trajectories is limited owing to suboptimal acquisition (see Limitations). Validation of the trajectories is difficult because of missing knowledge related to the true structural connections in individuals. Tracer studies have been used as a gold standard and have shown high resemblance of big white matter tracts in macaque monkeys.[41] However, especially at an individual level, the accuracy of small fibre bundles is limited.[42]

Limitations

A limitation of TMS studies in general is a lack of knowledge about optimal stimulation parameters[2] and the prolongation and durability of clinical effects.[43] Patients showing little clinical response at T4 (2 weeks after the stimulation protocol) might be slow responders. Indeed, previous studies[44,45] have shown that longer stimulation protocols might lead to remission in participants who did not remit initially. Because we

Table 2: Significant correlations* between clinical response and structural connectivity†‡

Metric, region	Correlation coefficient	*p* value	Slope
Number of tracts, right caudal cingulate cortex	0.41	0.02	5.46
Number of tracts, left posterior cingulate cortex	0.40	0.02	5.42
Volume of tracts, right caudal cingulate cortex	0.35	0.04	1329
Mean diffusivity, right caudal cingulate cortex	0.43	0.01	0.01

dTot = total distance.
*$p < 0.05$, uncorrected.
†Between the stimulation position in the left dorsolateral prefrontal cortex and the regions of interest in the cingulate cortex, represented by *dTot*, including *p* value and slope (Fig. 4).
‡Not all patients showed indirect connections between the stimulation site and the cingulate cortex.

have no information about the timing of the propagation of the TMS effects via structural connections to potentially cause clinical effects, the findings of this study might be different if clinical data were recorded at different time points.

In the statistical analysis, the stimulation order (sham–active v. active–sham) was not explicitly taken into account. Therefore, the time between the real TMS stimulation and assessment of the delayed clinical effects differed depending on which arm of the study the patients were in.

In this study, we used the diffusion tensor to perform tractography because of the limited ($n = 30$) number of diffusion gradients and the low b value (single shell, 800 s/mm^2). A well-known limitation of the diffusion tensor is resolving voxels that contain multiple fibre directions (i.e., kissing or crossing fibres).[46–48] This might have been why some connections were missing in some patients. In future studies, we recommend using multi-shell data with a higher range of b values[49] and a large number of gradient directions to achieve high angular resolution diffusion imaging,[50] although this puts pressure on study participants, because scanning time can increase drastically. Longer scans tend to increase the presence of artifacts, such as notable patient motion[51] and signal drift[23] due to gradient temperature changes. Recent developments in tractography suggest[52] that more advanced models than diffusion tensor imaging, such as diffusional kurtosis imaging,[53,54] constrained spherical deconvolution[55,56] or diffusion spectrum imaging,[57] should be taken into consideration.

We used 5 different metrics to quantify the structural connectivity strength between the stimulated left dlPFC and 9 ROIs in the cingulate cortex. This approach induced a multiple comparison issue. However, because this was the first study to investigate the potential for dMRI data to predict clinical response to aiTBS, we considered it to be exploratory, and all findings with $p < 0.05$ were reported.

Some patients without structural connections between the stimulation site and the ROIs in the cingulate cortex showed clinical improvement (Appendix 1). This might indicate that the clinical effects of aiTBS are at least not solely related to structural connectivity between the stimulation position and the cingulate cortex. Other limbic structures could be involved in the relief of depressive symptoms.[58,59]

Furthermore, the exact $dTot_{dlPFC-ROI}$ measure to quantify the structural connectivity between the dlPFC and any of the ROIs in the cingulate cortex was derived from the path-length formula[33] but has never been used before in this exact form. Validation of this measure in replication studies is therefore highly recommended. In accordance with Roge and colleagues[37] and Deligianni and colleagues,[38] we studied pathways up to 2 internodes. Given that more internodes results in more potential pathways, the direction of neuronal communication (orthodromic versus antidromic) cannot be derived from dMRI data. Therefore, this method has a high potential for including false pathways in the analysis pipeline.

The actual activation of neuronal white matter tracts by TMS depends on multiple factors, such as the TMS coil position and orientation, and the distance between the coil and the white matter tracts. For neuronal activation, there should be a component of the TMS-induced electric field that aligns with the white matter tract and exceeds an activation threshold.[2,60] Previous studies have demonstrated preferred sites of activation in the sulcal walls, where pyramidal cells bend and create high electric field gradients.[61] Future studies might benefit from combining electric field simulations with tractography to more accurately determine the actual activated neuronal pathways in the brain.[62,63]

Conclusion

This was the first study to investigate the biomarker potential of dMRI data to predict the clinical response to aiTBS. Structural connections between the patient-specific stimulation area in the left dlPFC and the right caudal and the left posterior part of the cingulate cortex were predictive for clinical outcomes. These findings were in line with our hypothesis that baseline structural connectivity may be of essence for clinical response to aiTBS in some patients, although the aiTBS protocol also induced positive clinical effects in patients who did not show these structural connections. Future research is necessary, including larger patient samples, to confirm these results. After validation of the potential of this dMRI-based prognostic biomarker, dMRI data might be used to optimize and personalize stimulation protocols.

Acknowledgements: D. Klooster and C. Baeken are supported by the Ghent University Multidisciplinary Research Partnership, "The integrative neuroscience of behavioral control," and a grant of the "Fonds Wetenschappelijk Onderzoek Rode Neuzen" (G0F4617N). K. Caeyenberghs is supported by a Career Development Fellowship from the National Health and Medical Research Council and an ACURF Program grant from the Australian Catholic University. The research of S. David and A. Leemans is supported by VIDI Grant 639.072.411 from the Netherlands Organization for Scientific Research (NWO).

Affiliations: From the Eindhoven University of Technology, Department of Electrical Engineering, Eindhoven, the Netherlands (Klooster, Vos, Besseling, Aldenkamp); the Academic Center for Epileptology Kempenhaeghe, Department of Research and Development, Heeze, the Netherlands (Klooster, Aldenkamp); Ghent

University, Ghent Experimental Psychiatry Laboratory, Ghent, Belgium (Baeken); the Australian Catholic University, Faculty of Health Sciences, Mary MacKillop Institute for Health Research, Melbourne, Australia (Caeyenberghs); the PROVIDI Lab, Image Sciences Institute, University Medical Center Utrecht and Utrecht University, Utrecht, the Netherlands (Leemans, David); the Brussel University Hospital, Department of Psychiatry, Brussels, Belgium (Baeken).

Competing interests: None declared.

Contributors: D. Klooster, R. Besseling, A. Aldenkamp and C. Baeken designed the study. C. Baeken acquired and analyzed the data, which D. Klooster, I. Vos, K. Caeyenberghs, A. Leemans and S. David also analyzed. D. Klooster and C. Baeken wrote the article, which all authors reviewed. All authors approved the final version to be published and can certify that no other individuals not listed as authors have made substantial contributions to the paper.

References

1. George MS, Taylor JJ, Short EB. The expanding evidence base for rTMS treatment of depression. *Curr Opin Psychiatry* 2013;26:13-8.
2. Klooster DCW, De Louw AJA, Aldenkamp AP, et al. Technical aspects of neurostimulation: focus on equipment, electric field modeling, and stimulation protocols. *Neurosci Biobehav Rev* 2016;65:113-41.
3. Berlim MT, Van Den Eynde F, Tovar-Perdomo S, et al. Response, remission and drop-out rates following high-frequency repetitive transcranial magnetic stimulation (rTMS) for treating major depression: a systematic review and meta-analysis of randomized, double blind and sham-controlled trials. *Psychol Med* 2014;44:225-39.
4. Baeken C, Vanderhasselt MA, Remue J, et al. Intensive HF-rTMS treatment in refractory medication-resistant unipolar depressed patients. *J Affect Disord* 2013;151:625-31.
5. Fitzgerald PB, Hoy KE, Elliot D, et al. Accelerated repetitive transcranial magnetic stimulation in the treatment of depression. *Neuropsychopharmacology* 2018;43:1565-72.
6. Baeken C, De Raedt R. Neurobiological mechanisms of repetitive transcranial magnetic stimulation on the underlying neurocircuitry in unipolar depression. *Dialogues Clin Neurosci* 2011;13:139-45.
7. Mayberg HSHS. Modulating dysfunctional limbic-cortical circuits in depression: towards development of brain-based algorithms for diagnosis and optimised treatment. *Br Med Bull* 2003;65:193-207.
8. Fox MD, Buckner RL, Liu H, et al. Resting-state networks link invasive and noninvasive brain stimulation across diverse psychiatric and neurological diseases. *Proc Natl Acad Sci U S A* 2014;111:E4367-75.
9. Lozano AM, Mayberg HS, Giacobbe P, et al. Subcallosal cingulate gyrus deep brain stimulation for treatment-resistant depression. *Biol Psychiatry* 2008;64:461-7.
10. Fox MD, Buckner RL, White MP, et al. Efficacy of TMS targets for depression is related to intrinsic functional connectivity with the subgenual cingulate. *Biol Psychiatry* 2012;72:595-603.
11. Weigand A, Horn A, Caballero R, et al. Prospective validation that subgenual connectivity predicts antidepressant efficacy of transcranial magnetic stimulation sites. *Biol Psychiatry* 2018;84:28-37.
12. Baeken C, De Raedt R, Van Hove C, et al. HF-rTMS Treatment in medication-resistant melancholic depression: results from 18FDG-PET brain imaging. *CNS Spectr* 2009;14:439-48.
13. Amico E, Bodart O, Rosanova M, et al. Tracking dynamic interactions between structural and functional connectivity: a TMS/EEG-dMRI study. *Brain Connect* 2017;7:84-97.
14. Le Bihan D, Mangin JF, Poupon C, et al. Diffusion tensor imaging: concepts and applications. *J Magn Reson Imaging* 2001;13:534-46.
15. Le Bihan D. Looking into the functional architecture of the brain with diffusion MRI. *Int Congr Ser* 2006;1290:1-24.
16. Sheehan DV, Lecrubier Y, Sheehan KH, et al. The Mini International Neuropsychiatric Interview (M.I.N.I): the development and validation of a structured diagnostic psychiatric interview for DSM-IV and ICD-10. *J Clin Psychiatry* 1998;59:22-33.
17. Duprat R, Desmyter S, Rudi DR, et al. Accelerated intermittent theta burst stimulation treatment in medication-resistant major depression: a fast road to remission? *J Affect Disord* 2016;200:6-14.
18. Peleman K, Van Schuerbeek P, Luypaert R, et al. Using 3D-MRI to localize the dorsolateral prefrontal cortex in TMS research. *World J Biol Psychiatry* 2010;11:425-30.
19. Leemans A, Jeurissen B, Sijbers J, et al. ExploreDTI: a graphical toolbox for processing, analyzing, and visualizing diffusion MR data. In: *Proceedings of the 17th Scientific Meeting of the International Society for Magnetic Resonance in Medicine*; 2009 Apr 18-24; Honolulu (HI). Concord (CA); International Society for Magnetic Resonance in Medicine; 2009: 3537.
20. Irfanoglu MO, Walker L, Sarlls J, et al. Effects of image distortions originating from susceptibility variations and concomitant fields on diffusion MRI tractography results. *Neuroimage* 2012;61:275-88.
21. Leemans A, Jones DK. The B-matrix must be rotated when correcting for subject motion in DTI data. *Magn Reson Med* 2009;61:1336-49.
22. Vos SB, Tax CMWW, Luijten PR, et al. The importance of correcting for signal drift in diffusion MRI. *Magn Reson Med* 2017;77:285-99.
23. Caeyenberghs K, Duprat R, Leemans A, et al. Accelerated intermittent theta burst stimulation in major depression induces decreases in modularity: a connectome analysis. *Netw Neurosci* 2019;3:157-72.
24. Caeyenberghs K, Leemans A, Coxon J, et al. Bimanual coordination and corpus callosum microstructure in young adults with traumatic brain injury: a diffusion tensor imaging study. *J Neurotrauma* 2011; 28:897-913.
25. Tax CMWW, Otte WM, Viergever MA, et al. REKINDLE: Robust Extraction of Kurtosis INDices with Linear Estimation. *Magn Reson Med* 2015;73:794-808.
26. Veraart J, Sijbers J, Sunaert S, et al. Weighted linear least squares estimation of diffusion MRI parameters: strengths, limitations, and pitfalls. *Neuroimage* 2013;81:335-46.
27. Basser PJ, Pajevic S, Pierpaoli C, et al. In vivo fiber tractography using DT-MRI data. *Magn Reson Med* 2000;44:625-32.
28. Tzourio-Mazoyer N, Landeau B, Papathanassiou D, et al. Automated anatomical labeling of activations in SPM using a macroscopic anatomical parcellation of the MNI MRI single-subject brain. *Neuroimage* 2002;15:273-89.
29. Fox MD, Liu H, Pascual-Leone A. Identification of reproducible individualized targets for treatment of depression with TMS based on intrinsic connectivity. *Neuroimage* 2013;66:151-60.
30. Valero-Cabré A, Payne BR, Rushmore J, et al. Impact of repetitive transcranial magnetic stimulation of the parietal cortex on metabolic brain activity: a 14C-2DG tracing study in the cat. *Exp Brain Res* 2005;163:1-12.
31. Hagmann P, Cammoun L, Gigandet X, et al. Mapping the structural core of human cerebral cortex. *PLoS Biol* 2008;6:e159.
32. Rubinov M, Sporns O. Complex network measures of brain connectivity: uses and interpretations. *Neuroimage* 2010;52:1059-69.
33. Watts DJ, Strogatz SH. Collective dynamics of "small-world" networks. *Nature* 1998;393:440-2.
34. Hamilton M. Development of a rating scale for primary depressive illness. *Br J Soc Clin Psychol* 1967;6:278-96.
35. Langguth B, Wiegand R, Kharraz A, et al. Pre-treatment anterior cingulate activity as a predictor of antidepressant response to repetitive transcranial magnetic stimulation (rTMS). *Neuroendocrinol Lett* 2007;28:633-8.
36. Honey CJ, Sporns O, Cammoun L, et al. Predicting human resting-state functional connectivity. *Proc Natl Acad Sci U S A* 2009;106:2035-40.
37. Roge R, Ambrosen KS, Albers KJ, et al. Whole brain functional connectivity predicted by indirect structural connections. In: *2017 IEEE international workshop on pattern recognition in neuroimaging (PRNI)*. 2017 Jun 21-23; Toronto, Canada. New York; IEEE; 2017. doi: 10.1109/PRNI.2017.7981496.
38. Deligianni F, Robinson E, Beckmann CF, et al. Inference of functional connectivity from direct and indirect structural brain connections. In: *2011 IEEE international symposium on biomedical imaging: from nano to macro*. 2011 Mar 30 to Apr 2; Chicago (IL). New York; IEEE; 2011. doi:10.1109/ISBI.2011.5872537.
39. Le Bihan D. Apparent diffusion coefficient and beyond: what diffusion MR imaging can tell us about tissue structure. *Radiology* 2013;268:318-22.
40. Alexander AL, Hurley SA, Samsonov AA, et al. Characterization of cerebral white matter properties using quantitative magnetic resonance imaging stains. *Brain Connect* 2011;1:423-46.
41. Schmahmann JD, Pandya DN, Wang R, et al. Association fibre pathways of the brain: parallel observations from diffusion spectrum imaging and autoradiography. *Brain* 2007;130:630-53.
42. Thomas C, Ye FQ, Irfanoglu MO, et al. Anatomical accuracy of brain connections derived from diffusion MRI tractography is inherently limited. *Proc Natl Acad Sci U S A* 2014;111:16574-9.

43. Senova S, Cotovio G, Pascual-leone A, et al. Durability of antidepressant response to repetitive transcranial magnetic stimulation: systematic review and meta-analysis. *Brain Stimul* 2019;12:119-28.
44. Stubbeman WF, Ragland V, Khairkhah R. Bilateral neuronavigated 20Hz theta burst TMS for treatment refractory depression: an open label study. *Brain Stimul* 2018;11:953-5.
45. McDonald WM, Durkalski V, Iii ERB, et al. Improving the antidepressant efficacy of transcranial magnetic stimulation: maximizing the number of stimulations and treatment location in treatment resistant depression. *Depress Anxiety* 2011;28:973-80.
46. Jeurissen B, Leemans A, Tournier JD, et al. Investigating the prevalence of complex fiber configurations in white matter tissue with diffusion magnetic resonance imaging. *Hum Brain Mapp* 2013;34:2747-66.
47. Jones DK, Knösche TR, Turner R. White matter integrity, fiber count, and other fallacies: the do's and don'ts of diffusion MRI. *Neuroimage* 2013;73:239-54.
48. Jones DK, Leemans A. Diffusion tensor imaging. *Methods Mol Biol* 2011;711:127-44.
49. Jeurissen B, Tournier JD, Dhollander T, et al. Multi-tissue constrained spherical deconvolution for improved analysis of multi-shell diffusion MRI data. *Neuroimage* 2014;103:411-26.
50. Mori S, Tournier D. Moving beyond DTI: high angular resolution diffusion imaging (HARDI). In: *Introduction to diffusion tensor imaging*. Amsterdam, Netherlands; Elsevier; 2013: 65-78.
51. Yendiki A, Koldewyn K, Kakunoori S, et al. Spurious group differences due to head motion in a diffusion MRI study. *Neuroimage* 2014; 88:79-90.
52. David S, Heemskerk AM, Corrivetti F, et al. The superoanterior fasciculus (SAF): a novel white matter pathway in the human brain? *Front Neuroanat* 2019;13:24.
53. Umesh Rudrapatna S, Wieloch T, Beirup K, et al. Can diffusion kurtosis imaging improve the sensitivity and specificity of detecting microstructural alterations in brain tissue chronically after experimental stroke? Comparisons with diffusion tensor imaging and histology. *Neuroimage* 2014;97:363-73.
54. Szczepankiewicz F, Lätt J, Wirestam R, et al. Variability in diffusion kurtosis imaging: impact on study design, statistical power and interpretation. *Neuroimage* 2013;76:145-54.
55. Sinke MRT, Otte WM, Christiaens D, et al. Diffusion MRI-based cortical connectome reconstruction: dependency on tractography procedures and neuroanatomical characteristics. *Brain Struct Funct* 2018;223:2269-85.
56. Tournier J-D, Mori S, Leemans A. Diffusion tensor imaging and beyond. *Magn Reson Med* 2011;65:1532-56.
57. Wedeen VJ, Wang RP, Schmahmann JD, et al. Diffusion spectrum magnetic resonance imaging (DSI) tractography of crossing fibers. *Neuroimage* 2008;41:1267-77.
58. Liu W, Ge T, Leng Y, et al. The role of neural plasticity in depression: from hippocampus to prefrontal cortex. *Neural Plast*. 2017; 6871089.
59. Greicius MD, Krasnow B, Reiss AL, et al. Functional connectivity in the resting brain: a network analysis of the default mode hypothesis. *Proc Natl Acad Sci U S A* 2003;100:253-8.
60. Wagner T, Valero-Cabre A, Pascual-Leone A. Noninvasive human brain stimulation. *Annu Rev Biomed Eng* 2007;9:527-65.
61. Nummenmaa A, NcNab JA, Savadjiev P, et al. Targeting of white matter tracts with transcranial magnetic stimulation. *Brain Stimul* 2014;7:80-4.
62. De Geeter N, Crevecoeur G. Leemans a, Dupré L. Effective electric fields along realistic DTI-based neural trajectories for modelling the stimulation mechanisms of TMS. *Phys Med Biol* 2015;60:453-71.
63. De Geeter N, Crevecoeur G, Dupré L, et al. A DTI-based model for TMS using the independent impedance method with frequency-dependent tissue parameters. *Phys Med Biol* 2012;57:2169-88.